

# Validation Studies for Concrete Constitutive Models with Blast Test Data

Youcai Wu, John E. Crawford, Shengrui Lan, Joseph M. Magallanes

*Karagozian & Case, 700 N Brand Blvd, Glendale, CA 91203*

## Abstract

*Many concrete constitutive models are available for use in LS-DYNA<sup>®</sup>. A thorough validation related to their applicability for the types of problems at hand should be made before application of any of these models. The process for validating a constitutive model includes examining the results produced with the model related to the behaviors it exhibits, gathering a suite of measured data collection pertinent to the problem to be addressed, and comparisons of measured and computed data. This paper addresses issues related to blast response analyses, which include simplification of boundary conditions (such as support condition and contact interfaces), numerical discretization, and material modeling. It was found important that the strain rate effects should be imposed properly since blast loadings usually excite high frequency and high strain rate responses. The impact of boundary conditions was also identified through the numerical studies.*

Keywords: concrete constitutive modeling, blast response, strain rate effects, contact algorithm

## 1. Introduction

The safety of reinforced concrete structures subjected to blast loads is sometimes a major concern in the design of new structures or the retrofitting of old ones. Full-scale structural tests are very costly and making it impractical for the most part to conduct experiments with blast loads. Therefore, physics-based numerical analysis has been an important approach for civil engineers to determine the behaviors of reinforced concrete (RC) structures under blast loads. Given a proper modeling approach, LS-DYNA has shown its great potential in performing such analyses for structural responses under blast loads.

In these situations, physics-based constitutive models have shown great promises to generate physical responses numerically. Although it is very difficult to predict the behavior of concrete exactly, if not impossible, the constitutive model should be able to capture the most basic behaviors of concrete. LS-DYNA provides a good library of concrete constitutive models, such as, Mat\_Concrete\_Damage\_Rel3 (KCC Model or MAT072R3 [4, 7]), Mat\_Winfrith\_Concrete (Winfrith model or MAT084 [1]), Mat\_CSCM\_Concrete (CSC Model or MAT159 [8, 10]), and Mat\_RHT (RHT model or MAT272, [9]). The keyword input for these models is relatively simple and each of them provides a parameter automatic generation version.

The fundamental performances of the aforementioned constitutive models have been investigated in previous works [4, 11]. The focus of this work is to evaluate the four constitutive models through comparison of their blast responses. This is done through numerical analyses of a reinforced concrete slab subjected to blast loadings. The numerical responses are compared

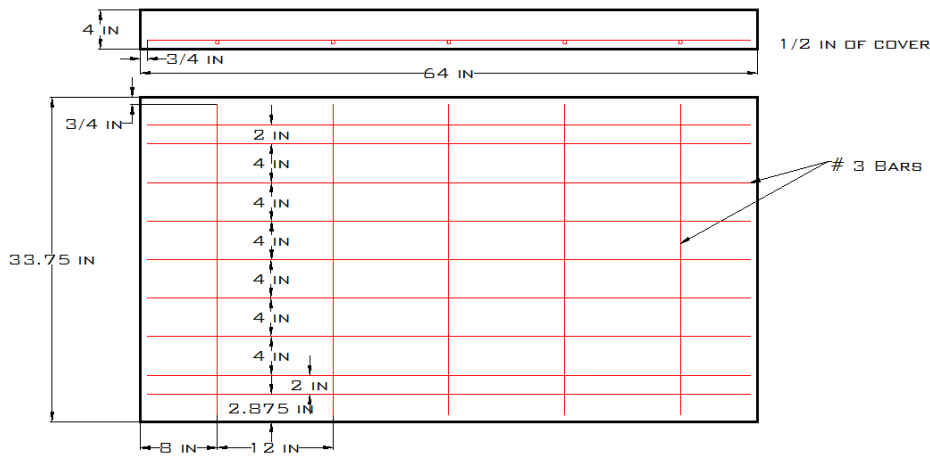
with experimental data so that the effectiveness of each model can be evaluated, and the importance of such factors as boundary conditions and rate enhancement can be clarified. The code used for the numerical studies is LS-DYNA version “smp d R7.0.0” Revision 79055, released on 1/10/2013; basic inputs are used for all the material models.

## 2. Test setup

Recently (<http://sce.umkc.edu/blast-prediction-contest/home.html>), a suite of blast tests of RC slabs were conducted at the Engineering Research and Development Center (ERDC), Vicksburg, Mississippi using the Blast Loading Simulator (BLS). The BLS is capable of simulating a uniform blast-like pressure on the face of slab. Both positive and negative phases of the pressure can be captured. Data captured included pressures at six different locations, a central accelerometer and laser deflection measurements on the back face.

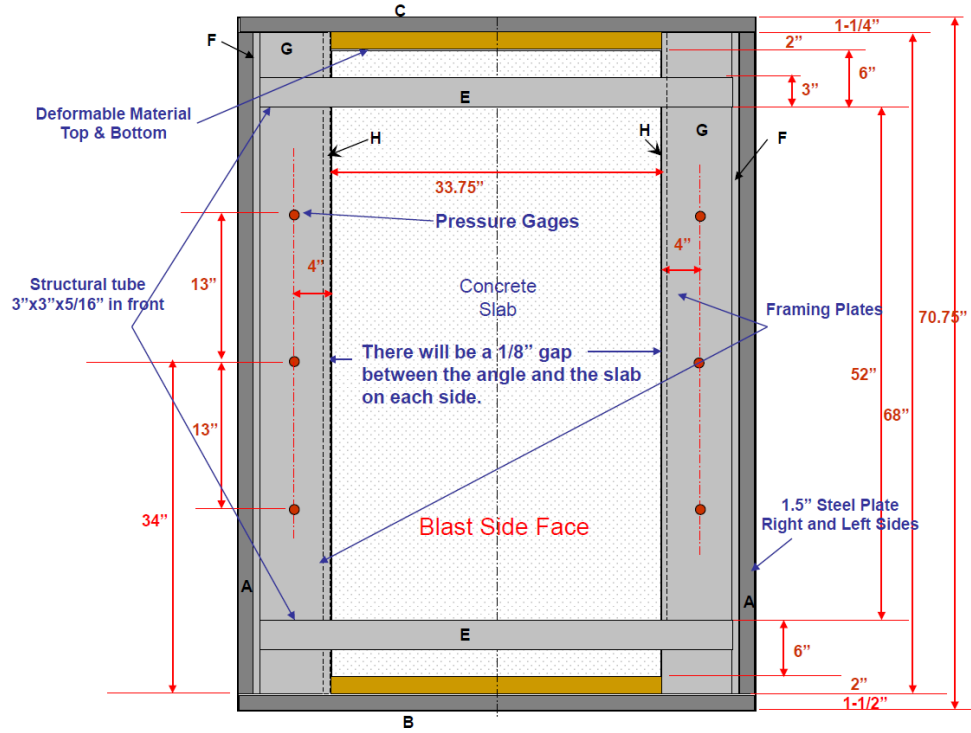
One of these tests is selected as the example problem in this study to investigate the factors that contribute to the numerical prediction of the response of a structure when subjected to shock/blast loadings. These factors include boundary conditions; complexity of material properties available; material models used; and finite element parameters, such as element type selection, mesh size sensitivity, and material model rate effects amongst others. In this study, particular attention is paid to the material model rate effects and boundary conditions.

A drawing of the RC slab considered and the geometry of the test specimen and setup are shown in Figure 1. The slab has a thickness of 4.0 inches, width of 33.75 inches, and height of 64 inches. The slab is reinforced by #3 rebars as shown. The unconfined compressive strength of the concrete is 5 ksi and the reinforcement is Gr.60 steel. The averaged pressure obtained (from the 6 pressure gauges) is shown in Figure 2.



LONGITUDINAL BARS = 62.5 IN  
 HORIZONTAL BARS = 32.35 IN

(a) Drawings of the slab



(b) Geometry of the testing platform

Figure 1. Test setup (<http://sce.umkc.edu/blast-prediction-contest/home.html>)

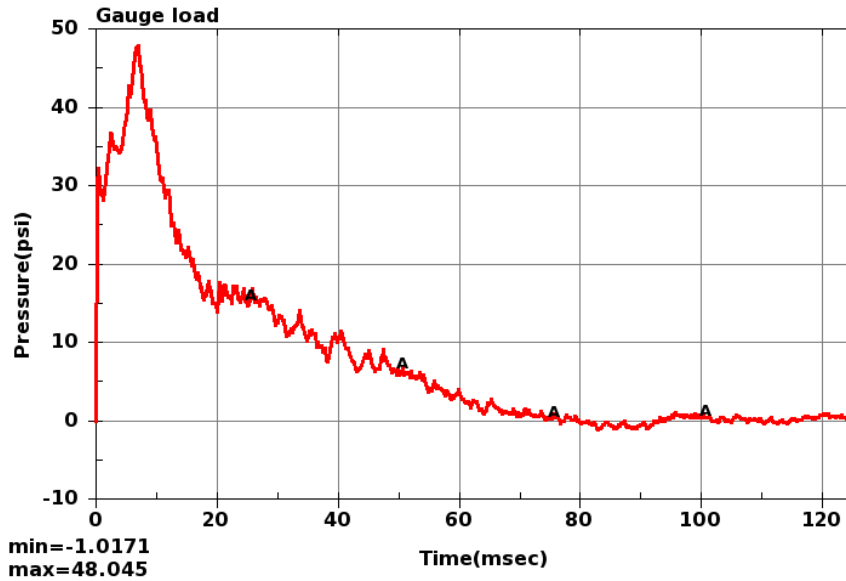


Figure 2. Averaged pressure from pressure gauges

### 3. Numerical discretization

The LS-DYNA model used for the finite element analyses of the RC slab is shown in Figure 3. The concrete in the slab is discretized by 1 inch cubic solid elements; the reinforcement is modeled by 1 inch (length) Hughes-Liu beam elements sharing nodes with the concrete. The structural tubes used by the reaction structure to support the slab are discretized by 1 inch squared shell elements; the top and bottom support frames are modeled by 1 inch cubic solid elements as well.

For the material modeling, the concrete is modeled by the aforementioned four constitutive models with constant stress elements. The Gr.60 reinforcement is modeled using a piecewise linear plasticity model, and the structural tubes and support frames are modeled as ASTM A36 steel with a piecewise linear plasticity model. Viscous type hourglass control is applied to mitigate the effects of the zero energy modes since the load is a high frequency dynamic load.

The two ends of the structural tubes are fixed and the support frames are fixed at their back face, as can be seen in Figure 3(b). Contact interfaces are defined between the slab and the structural tubes and support frames. Single surface contact is defined between the slab and the structural tubes and support frames using a coefficient of friction (COF) of 0.25 for the most part. Results for other COF values are also shown. The pressure histories shown in Figure 2 is applied uniformly over the front face of the slab since the BLS is capable of generating a uniform pressure on the blast face.

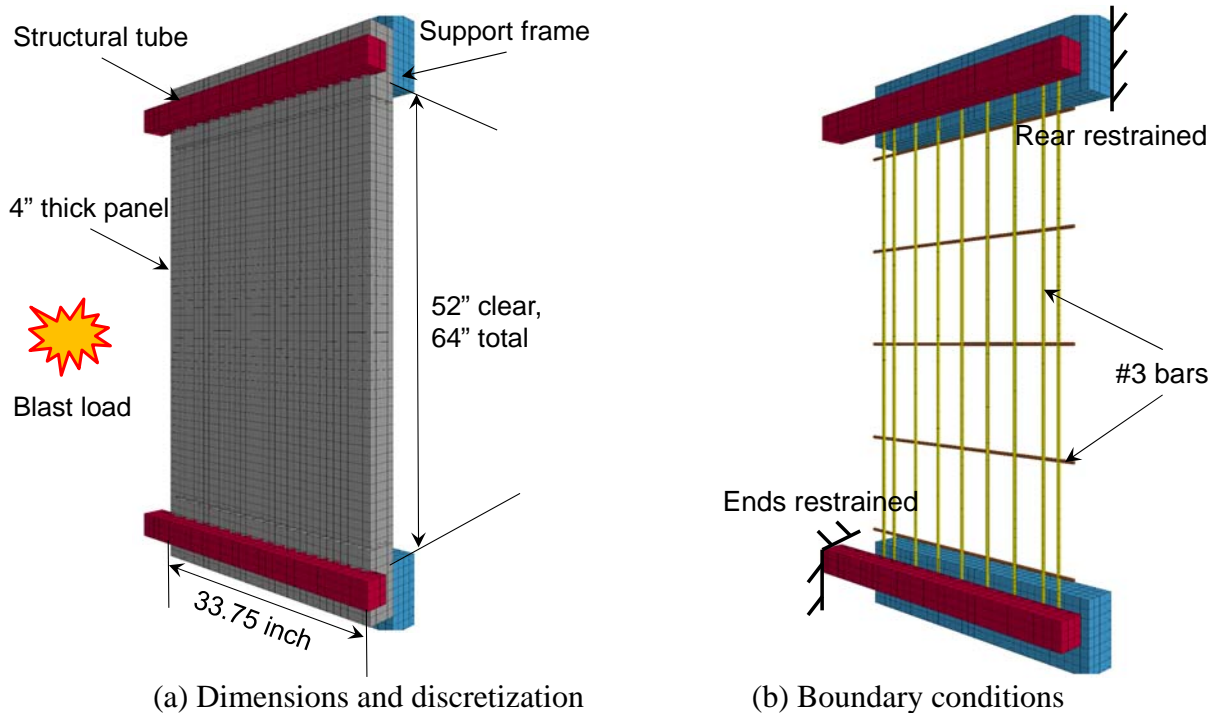


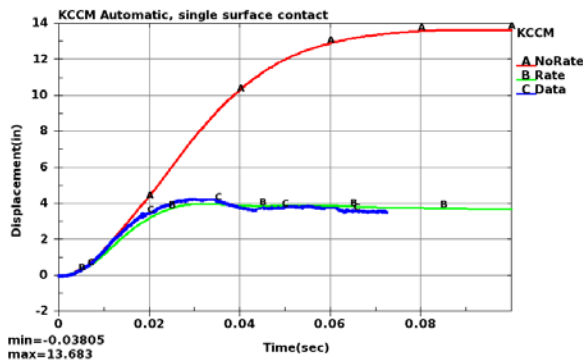
Figure 3. FE model for the RC slab considered

### 4. Numerical results

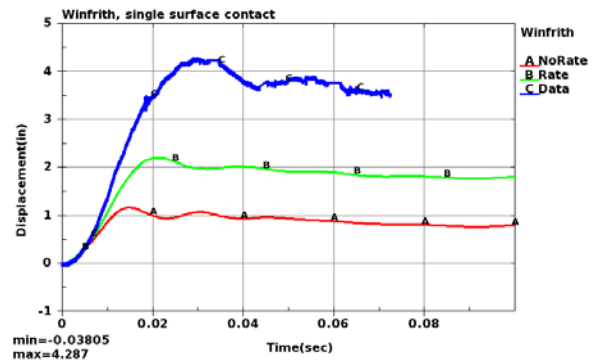
#### 4.1. Strain rate effect

Experimental data [2, 4] have shown that concrete strength has strain rate dependence, therefore, the strain rate enhancement should be applied when the strain rate is high, as is the case with a blast loading. Comparisons of the computed mid-height lateral deflections against test data for the four constitutive models, with and without rate enhancement, are shown in Figure 4. Rate effects are handled differently by the concrete models considered. The KCC model uses a rate effects curve (input externally to the KCC model itself, which is taken from a paper by Malvar [6] and presented in the appendix where negative implies tensile rates) to enhance concrete strength with strain rate, while the CSC and Winfrith models seem to use an internal enhancement. For the RHT model, the rate enhancement depends on the reference strain rate (EOC and EOT) on the input cards. For example, the reference rate is  $EOC/EOT=10^{-9}$  for the result shown. However, if the reference rate is  $EOC/EOT=10^{-6}$ , adverse effect might be observed.

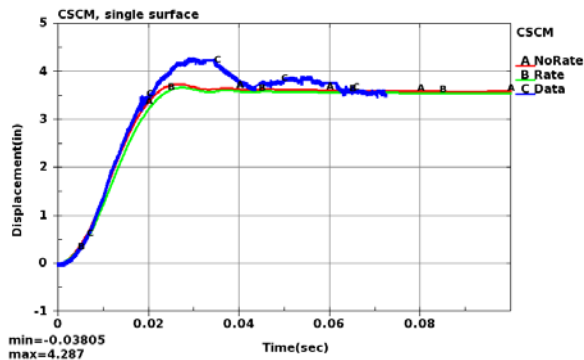
Using the KCC model, the deflection matches test data very well when the rate effects are modeled appropriately, and when these are ignored, a huge discrepancy exists. It is worth noting that automatically generated parameters (as any analyst can do without knowing too much about the concrete, input cards shown in appendix) are used for the KCC model, as indicated in the appendix. The CSC model shows negligible influence from rate effects and the results agree with test data quite well. The opposite effect is observed for the Winfrith model since the deflection is smaller when the rate effect is not applied (RATE=1 on the input card), which seems at odds with experimental measurements and the literature on the subject. RHT model significantly underpredicts the deflection. In addition, the initial stiffness is not captured by the Winfrith and RHT models.



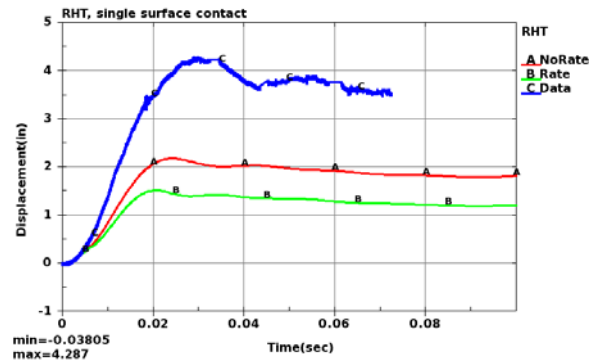
(a) KCC Model



(b) Winfrith Model



(c) CSC Model



(d) RHT Model

Figure 4. Lateral deflection histories at central mid-height on back face

4.2. Boundary conditions

The friction between the slab and the structural tubes and support frames could play an important role in the responses of the slab. For example, if the friction is infinite (i.e., the slab is tied to the tubes and frames), an arching effect will be built up and hence a high compressive-membrane effect could be generated. On the other hand, if it is frictionless, no compressive-membrane resistance could be built up and the tubes and frames could only provide constraints on the lateral deflection.

Figure 5 shows the lateral deflection histories for the four concrete models with various coefficients of friction (COFs) and with strain rate effects enforced and parameters automatically generated for all the models. Surface to surface contacts are defined between the slab and the tubes and frames. Apparent influences are observed for the COFs for all the models. It is seen that the KCC model and CSC model results match test data well when the COF is relatively high (0.25 or more), but the Winfrith and RHT results tend to agree with test data better when the COF is low or nearly zero. However, it should be pointed that the COF between concrete and steel is generally reported to be around 0.45 for quasi-static loads (<http://www.supercivilcd.com/FRICTION.htm>). The COF should not be reduced significantly in this test since the peak vertical velocity of the slab during the test is only about 40 in/sec.

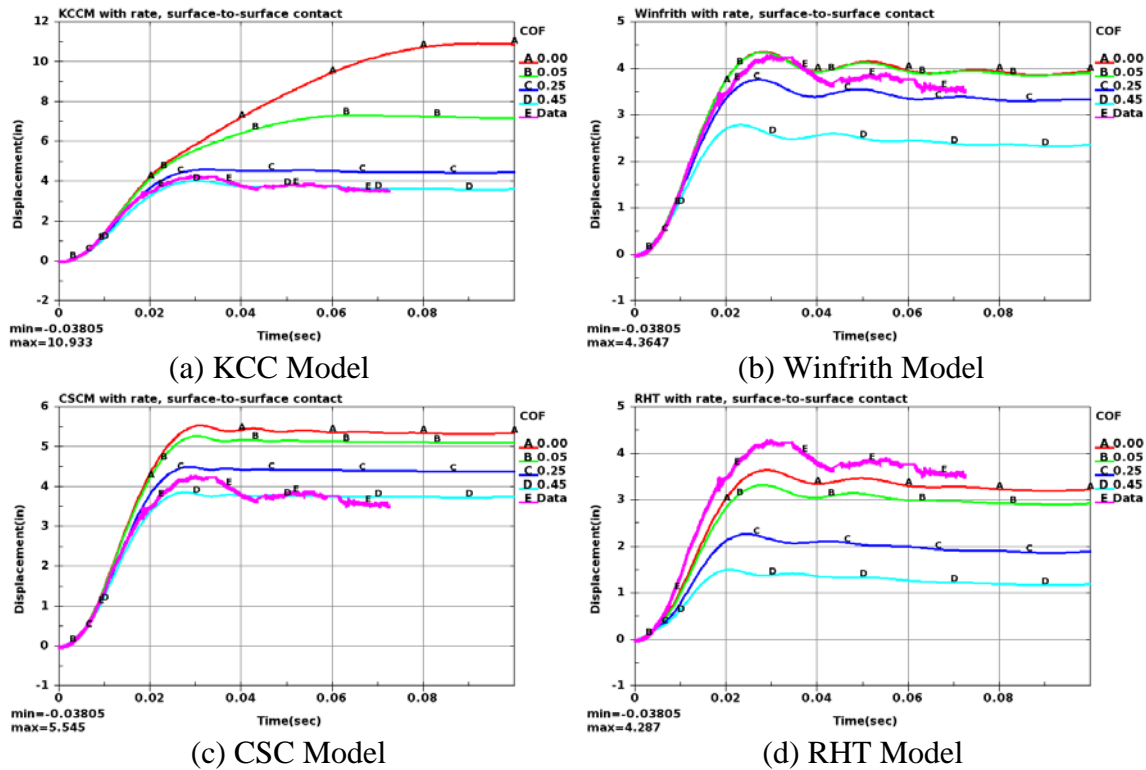


Figure 5. Lateral deflection histories for various coefficients of friction

### 4.3. Contact algorithms

Many contact algorithms have been implemented into LS-DYNA, such as node to surface contact, surface to surface contact, and single surface contact, etc. The analyst needs to select a proper one from those available. Although they are expected to work equivalently, actually, they do not. For blast responses, single surface or surface to surface contact is usually preferred.

Figure 6 shows the deflection histories for single surface and surface to surface contact algorithms for the four concrete models with strain rate enhancement applied and automatic parameter generation used for all the models. The coefficient of friction is 0.25. In these situations, at least 20% difference between the two contact algorithms is observed for each of the four material models. The disparity between the two contact algorithms is particularly pronounced for the Winfrith model.

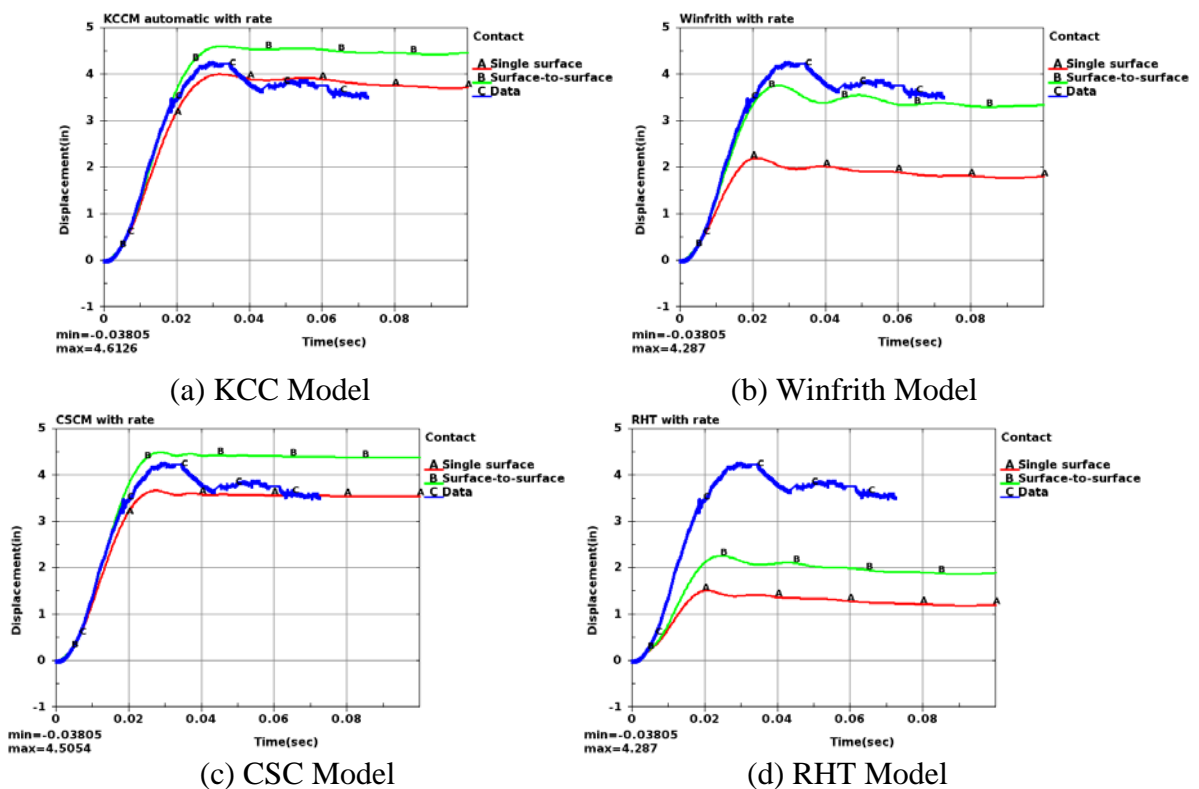


Figure 6. Lateral deflection histories for various contact algorithms

## 5. KCC model parameters

The KCC model has been widely used in the analyses for structural response of reinforced and unreinforced concrete structural components subjected to high frequency dynamic loads such as blast and impact loading. Some of the key parameters that could dramatically affect the numerical results are explained in this section.

### 5.1. Strain rate enhancement

It was shown in Section 4.1 that the rate enhancement is important for the KCC model if it is to effectively capture high strain rate events, which has been repeatedly demonstrated in benchmark comparisons with blast effects experiments. Any engineer can use the KCC model without knowing too much about concrete by using the automatic parameter generation version,

just as the one shown in this paper. Unfortunately, the automatic generation feature does not apply to dynamic increase factor (DIF) in the current LS-DYNA code. To activate the strain rate effect, the user needs to input a nonzero number under “LCRate” (see appendix) and define a load curve with LCID=LCRate. The DIF curve (see appendix) can be defined according to the following formulations. Note that positive values for strain rate are for compression and negative values are for tension.

According to CEB data [2], the compression DIF can be calculated by:

$$DIF_c = \begin{cases} \left( \frac{\dot{\epsilon}}{\dot{\epsilon}_s} \right)^{1.026\alpha} & \dot{\epsilon} \leq 10^6 / \text{sec} \\ \gamma \left( \frac{\dot{\epsilon}}{\dot{\epsilon}_s} \right)^{1/3} & \dot{\epsilon} > 10^6 / \text{sec} \end{cases} \quad (1)$$

with

$$\gamma = 10^{6.156\alpha-2} \quad (2)$$

$$\alpha = \frac{1}{5 + 9f'_c / f'_{co}} \quad (3)$$

where  $\dot{\epsilon}$  is the current strain rate,  $\dot{\epsilon}_s = 3 \times 10^{-5} / \text{sec}$  is the reference strain rate (treated as static),  $f'_c$  is the unconfined compressive strength of the concrete, and  $f'_{co} = 1450 \text{ psi}$ . Magallanes et al [5] suggest that the second branch of the strain rate effect showed in CEB data should be ignored.

According to Crawford and Malvar [3, 6], the tension DIF can be calculated by:

$$DIF_t = \begin{cases} \left( \frac{\dot{\epsilon}}{\dot{\epsilon}_s} \right)^\delta & \dot{\epsilon} \leq 1.0 / \text{sec} \\ \beta \left( \frac{\dot{\epsilon}}{\dot{\epsilon}_s} \right)^{1/3} & \dot{\epsilon} > 1.0 / \text{sec} \end{cases} \quad (4)$$

with

$$\beta = 10^{6\delta-2} \quad (5)$$

$$\delta = \frac{1}{1 + 8f'_c / f'_{co}} \quad (6)$$

where  $\dot{\epsilon}$  is the current strain rate,  $\dot{\epsilon}_s = 10^{-6} / \text{sec}$  is the reference strain rate (treated as static).

## 5.2. Damage evolution parameters

Concrete under little to moderate confinement exhibits strain softening, therefore, mesh dependence is unavoidable if no treatment is taken to mitigate it. There are three parameters combined together in the KCC model to control the damage evolution. These parameters are: B1, B2, and Omega (shown as “A0F” in the appendix for the input). B1 is the parameter that controls compressive damage evolution, B2 is the one that controls tensile damage evolution,

and Omega controls volume expansion. According to Crawford et al [4], to regularize the compression softening, B1 can be calculated as:

$$b_1 = 0.34h + 0.79 \tag{7}$$

where  $h$  is the characteristic length of the element in the units of “inch”. However, to apply this equation, the localization width  $w_{lz}$  (“LocWidth” on the input cards) should be set to smaller than the element size (no matter what the real aggregate size is).

According to Malvar’s work (not published), B2 should be calculated by:

$$b_2 = (0.09 * w_{lz}^2 - 0.98 * w_{lz} + 3.06)(1 - 0.004 * f_c'^2 + 0.097 * f_c' - 0.484) \tag{8}$$

where  $w_{lz}$  is the localization width in the units of “inch”,  $f_c'$  is the unconfined compressive strength in the units of “ksi”.

Furthermore, Omega is the parameter that governs the volume expansion, which has substantial influence on the structural responses, especially when confinement is present. According to Crawford et al [4], the suggested value for a situation without confinement is 0.75 and for a confined case is 0.90.

The above mentioned damage evolution parameters should be adjusted completely (i.e., B1, B2, and Omega all adjusted), if performed. Otherwise, as has demonstrated in the previous sections, the default combination of these parameters could predict a reasonable result as well if the strain rate enhancement is imposed properly.

Figure 7 shows the effect of the combinations of the damage evolution parameters. In Figure 7(a), Omega=0.5 for all the calculations. In Figure 7(b), B1=1.12 (Eq.(7)) and B2=1.96 (Eq.(8)) for all the calculations. Curve A in Figure 7(a) is from the default setup, and Curve B in Figure 7(b) is from the complete adjusted setup. It can be concluded that both the default and the complete adjusted parameters work effectively for this problem. It should also be pointed out that, in the numerical analyses, rate enhancement is activated and surface to surface contact algorithm is applied with the coefficient of friction being 0.45.

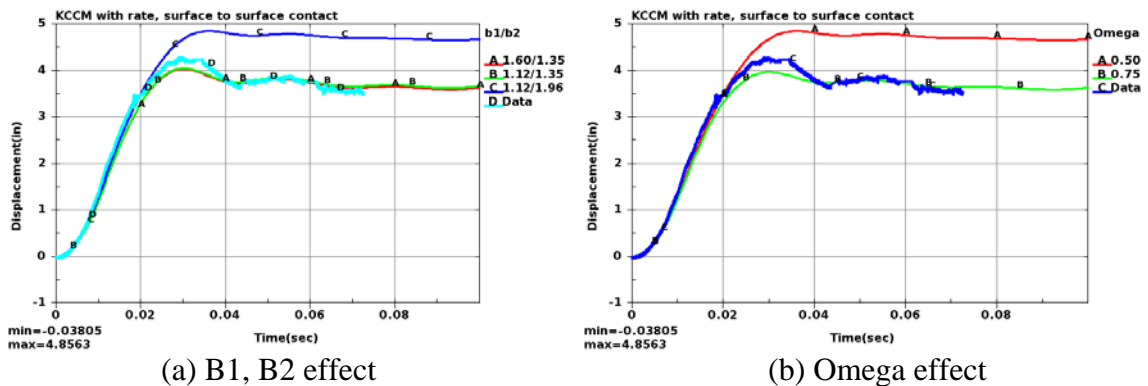


Figure 7. Lateral deflection histories for various damage evolution parameters

## 6. Conclusions

Four concrete constitutive models, namely, KCC, Winfrith, CSC, and RHT models of the several available in LS-DYNA are evaluated in this paper as to their capability to perform blast response calculations. It was found that the strain rate enhancement is very significant for the KCC model in analyzing and capturing blast effects responses. The influence of rate effect is not as important for the RHT model, and it is nearly nonexistent for the CSC model. In the case of the Winfrith model, its influence is inexplicably the opposite of that expected.

The study also showed that the boundary condition, specifically, the friction between the slab and the supporting structures, affects the numerical results dramatically. The KCC and CSC models work reasonably well in the near realistic range (i.e., COF=0.25~0.45), but the Winfrith and RHT models seem to work better for an unrealistically low COF (close to 0.0).

Another finding is that the contact algorithm also affects the numerical results. It is seen that at least 20% difference is exhibited for the results predicted by single surface contact algorithm as compared to those of the surface to surface contact algorithm. This indicates some more study should be done by LSTC to check the contact algorithms.

Finally, for users of the KCC model, it is highly recommended that the strain rate enhancement be activated for most analyses, even quasi-static ones, since strain rate effects can have a profound effect and often underappreciated effect on the responses. We recommend do so using the DIF curve populated using the formulations provided (Eqs.(1) and (4)). Other than this, the automatic parameter generation can still be applied to generate meaningful results.

## References:

1. Broadhouse, B.J. "The Winfrith concrete model in LS-DYNA3D," Safety Performance Department, Atomic Energy Authority Technology, Winfrith, SPD/D(95)363, February, 1995
2. Comite Euro-International du Beton - Federation Internationale de la Precontrainte, CEB-FIP Model Code 90 (ISBN 0-7277-1696-4), Redwood Books, Trowbridge, Wiltshire, Great Britain, 1990
3. Crawford J.E. and Malvar L.J. "User's and Theoretical Manual for K&C Concrete Model," Technical report TR-97-53.1, Karagozian & Case, Glendale, CA, 1997
4. Crawford, J.E., Wu, Y., Choi H.J., Magallanes, J.M., and Lan, S. "User's manual and documentation for release III of the K&C concrete material model in LS-DYNA," Technical Report TR-11-36.6, Karagozian & Case, Glendale, CA, November, 2011
5. Magallanes, J.M., Wu, Y., Malvar, L.J., and Crawford, J.E. "Recent Improvements to Release III of the K&C Concrete Model", *11<sup>th</sup> International LS-DYNA Users Conference*, Dearborn, MI, June 6-8, 2010
6. Malvar, L.J. and Crawford J.E. "Dynamic increase factors for concrete," *Twenty-Eighth DDESB Seminar*, Orlando, Florida, August, 1998
7. Malvar, L.J., Crawford, J.E., Wesevich, J.W., and Simons, D. "A plasticity concrete material model for DYNA3D," *International Journal of Impact Engineering*, vol. **19**, p847-873, 1997
8. Murray, Y.D., "Users manual for LS-DYNA concrete material model 159," Report No. FHWA-HRT-05-062, Federal Highway Administration, 2007

9. Riedel, W., Thomas, K., Hiermaier, S., and Schmolinske, E. "Penetration of Reinforced Concrete by BETA-B-500 Numerical Analysis Using a New Macroscopic Concrete Model for Hydrocodes," *9<sup>th</sup> International Symposium on Interaction of the Effects of Munitions with Structures*, p315-322, Berlin, Germany, May 3-7, 1999
10. Schwer, L.E., and Murray, Y.D. "A three-invariant smooth cap model with mixed hardening," *International Journal for Numerical and Analytic Methods in Geomechanics*, vol. **18**, p657-688, 1994
11. Wu Y., Crawford J.E., and Magallanes J.M. "Performance of LS-DYNA concrete constitutive models," *12<sup>th</sup> International LS-DYNA Users Conference*, Detroit, June 3-5, 2012

Appendix

Example input for the KCCM and its dynamic increasing factor curve:

```

*MAT_CONCRETE_DAMAGE_REL3
$ MATID RO PR
 72105000 2.120E-04 0.00E+00
$ f't A0 A1 A2 B1 AOF A1F
 0.00E+00 -5.000E+3 0.00E+00 0.00E+00 0.000 0.00 0.00E+00
$ sLambda NOUT EDROP RSIZE UCF LCRate LocWidth NPTS
 0.00E+00 0.00E+00 0.00E+00 00.00 0.00E+00 7210 0.00E+00 0.00e0
$ Lambda01 Lambda02 Lambda03 Lambda04 Lambda05 Lambda06 Lambda07 Lambda08
 0.00E+00 0.00E+00 0.0E-00 0.00E+00 0.00E+00 0.00E+00 0.00E+00 0.00E+00
$ Lambda09 Lambda10 Lambda11 Lambda12 Lambda13 B3 A0Y A1Y
 0.00E+00 0.00E+00 0.000e0 0.000e0 0.000e0 0.00E+00 0.00E+00 0.00E+00
$ Eta01 Eta02 Eta03 Eta04 Eta05 Eta06 Eta07 Eta08
 0.00E+00 0.00E+00 0.00E+00 0.00E+00 0.000E+0 0.00E+00 0.00E+00 0.00E+00
$ Eta09 Eta10 Eta11 Eta12 Eta13 B2 A2F A2Y
 0.00E+00 0.00E+00 0.00E+00 0.00E+00 0.000E+0 0.00E+00 0.00E+00 0.00E+00

*DEFINE_CURVE
$ LCID SIDR SFA SFO OFFA OFFO DATYYP
 7210 0 1.0 1.00
$ Strain-Rate Enhancement
-3.0000000E+04 1.0854217E+01
-3.0000000E+02 1.0854217E+01
-1.0000000E+02 7.5258937E+00
-3.0000000E+01 5.0380812E+00
-1.0000000E+01 3.4932103E+00
-3.0000000E+00 2.3384702E+00
-1.0000000E+00 1.6214048E+00
-1.0000000E-01 1.4959240E+00
-9.9999998E-03 1.3801543E+00
-1.0000000E-03 1.2733439E+00
-9.9999997E-05 1.1747997E+00
-9.9999997E-06 1.0838817E+00
0.0000000E+00 1.0000000E+00
2.9999999E-05 1.0000000E+00
9.9999997E-05 1.0348747E+00
1.0000000E-03 1.1049955E+00
9.9999998E-03 1.1798675E+00
1.0000000E-01 1.2598126E+00
1.0000000E+00 1.3451747E+00
3.0000000E+00 1.3879174E+00
1.0000000E+01 1.4363207E+00
3.0000000E+01 1.4819596E+00
1.0000000E+02 1.5336425E+00
3.0000000E+02 1.5823737E+00
3.0000000E+04 1.8040748E+00
    
```